NeuroImage 292 (2024) 120612

Contents lists available at ScienceDirect

NeuroImage

journal homepage: www.elsevier.com/locate/ynimg

Out-of-phase transcranial alternating current stimulation modulates the neurodynamics of inhibitory control

Jeehye Seo [a,b], Jehyeop Lee [b,c], Byoung-Kyong Min [a,b,c,*]

[a] Institute of Brain and Cognitive Engineering, Korea University, Seoul 02841, Korea
[b] BK21 Four Institute of Precision Public Health, Korea University, Seoul 02841, Korea
[c] Department of Brain and Cognitive Engineering, Korea University, Seoul 02841, Korea

ARTICLE INFO

Keywords:
Functional MRI
Inhibitory control
Non-invasive neuromodulation
Phase lagging
Transcranial alternating current stimulation

ABSTRACT

Transcranial alternating current stimulation (tACS) is an efficient neuromodulation technique that enhances cognitive function in a non-invasive manner. Using functional magnetic resonance imaging, we investigated whether tACS with different phase lags (0° and 180°) between the dorsal anterior cingulate and left dorsolateral prefrontal cortices modulated inhibitory control performance during the Stroop task. We found out-of-phase tACS mediated improvements in task performance, which was neurodynamically reflected as putamen, dorsolateral prefrontal, and primary motor cortical activation as well as prefrontal-based top-down functional connectivity. Our observations uncover the neurophysiological bases of tACS-phase-dependent neuromodulation and provide a feasible non-invasive approach to effectively modulate inhibitory control.

1. Introduction

Inhibitory control is a fundamental component of cognitive function because it empowers individuals to purposefully regulate their thoughts, behaviors, and responses (Friedman and Miyake, 2004; Strauss et al., 2006). Its significance lies in the several key aspects of cognitive processing. First, inhibitory control facilitates seamless switching between different tasks and mental processes, promoting the cognitive flexibility necessary for effective problem solving and adaptation to changing environments (Hendry et al., 2022). Additionally, it enables selective attention, allowing individuals to focus on relevant information while suppressing distractions (Diamond, 2013; Theeuwes, 2010). Inhibitory control is crucial for suppressing responses and inhibiting impulsive or inappropriate reactions (Diamond, 2013). This function enhances the effectiveness of working memory by filtering out irrelevant information (Friedman and Miyake, 2004). Moreover, inhibitory control is integral to goal-directed behavior, emotional regulation, and risk management, ensuring individuals stay aligned with their objectives and make well-considered decisions (Diamond, 2013; Fox and Calkins, 2003).

To execute appropriate behaviors and cognitive processes based on task demands, cognitive control, including selective attention, is necessary for controlled and coordinated action. Through selective attention, cognitive interference or competing information processing demands are reduced, and inappropriate habitual actions or interference are simultaneously suppressed (Miller and Cohen, 2001). However, with a strong distractor, it may be challenging to process task-relevant information and cognitive conflict may occur (Nee et al., 2007).

The Stroop task is a well-established psychological test that assesses an individual's ability to demonstrate cognitive and inhibitory control over automatic or habitual responses (Stroop, 1935). The classic Stroop task involves presenting participants with a list of color names (e.g., red, green, blue) written in incongruent ink colors (e.g., the word "red" written in blue ink). The participants are typically instructed to name the ink color as quickly and accurately as possible while ignoring the actual written word. This creates a conflict between the automatic processing of words and task-relevant information, which is the color of ink (Guo et al., 2018; Purmann and Pollmann, 2015). Inhibitory control, as demonstrated by the Stroop task, refers to the ability to suppress or override prepotent or automatic responses in favor of a more controlled and task-relevant response (Strauss et al., 2006). In the context of the Stroop task, inhibitory control is required to inhibit the automatic tendency to read a word and instead focus on identifying and naming the ink color (Siegrist, 1997).

Functional neuroimaging studies have identified several frontal

* Corresponding author at: Department of Brain and Cognitive Engineering, Director, Institute of Brain and Cognitive Engineering, Korea University, Seoul 02841, Korea.
E-mail address: min_bk@korea.ac.kr (B.-K. Min).

https://doi.org/10.1016/j.neuroimage.2024.120612
Received 19 January 2024; Received in revised form 25 March 2024; Accepted 12 April 2024
Available online 20 April 2024

brain regions that support cognitive control in the Stroop task, particularly the left dorsolateral prefrontal cortex (L-dlPFC) and the dorsal anterior cingulate cortex (dACC) (Banich et al., 2001; Krug and Carter, 2012; MacDonald et al., 2000; Menon and D'Esposito, 2022; Nee et al., 2007). The L-dlPFC maintains a representation of task-related demands, controls visual processes, and directs attention to pertinent features of stimuli (Banich et al., 2000, 2001; Egner and Hirsch, 2005; Polk et al., 2008). Furthermore, it plays a crucial role in exerting control over behavior with extensive connections to the sensory and motor regions (Miller and Cohen, 2001; Vanderhasselt et al., 2009). Increased dlPFC activity is observed during high-conflict trials in inhibitory control tasks such as the Stroop task, correlating with better behavioral performance (Silton et al., 2010). The dACC is also involved in conflict monitoring (Apps et al., 2012; Borsa et al., 2018; Yeung et al., 2004) and attentional inhibitory regulation processing (Johnston et al., 2007; Silton et al., 2010). Activity in this region closely mirrors the level of control recruited in conflict scenarios and has a strong functional relationship with the lateral prefrontal cortex (Botvinick, 2007; Botvinick et al., 2004; Kerns et al., 2004). Alongside the dACC, the dlPFC contributes to conflict induced behavioral adjustments, especially in tasks involving conflicting rules or responses, including the Stroop task (MacLeod and MacDonald, 2000).

On the other hand, non-invasive neuromodulation of cognitive control processes might impact cognitive performance augmentation. Various studies have used non-invasive brain stimulation methodologies, such as transcranial magnetic stimulation (TMS), direct current stimulation (tDCS), or alternating current stimulation (tACS) (Levasseur-Moreau and Fecteau, 2012; Mansouri et al., 2019; Pulopulos et al., 2020; Veniero et al., 2019). Furthermore, several studies have attempted to understand the causal influence of specific brain oscillations on cognitive function (Filmer et al., 2014; Herrmann et al., 2013; Thut and Miniussi, 2009). By utilizing these approaches and manipulating specific stimulation parameters, researchers have successfully demonstrated intentional modulation of brain activity as well as improved performance in cognitive tasks such as working memory performance (Brunoni and Vanderhasselt, 2014; Brunye et al., 2017; Hill et al., 2019; Kim et al., 2022) or inhibitory control (Schluter et al., 2018; Volpe et al., 2022). For example, neuronal communication relies on the coherent oscillation of activated neuronal groups, enabling effective interactions through synchronized communication windows and supporting cognitive flexibility (Fries, 2005). Using tACS to synchronize intrinsic neuronal oscillations to the applied stimulation phase, it is possible to effectively entrain brain rhythms through phase specificity (Johnson et al., 2020; Krause et al., 2019). To improve cognitive functions such as attention, executive skills, and context processing, phase synchronization is a crucial neuronal mechanism that manages intrinsic communication among distinct nodes (Doesburg et al., 2009; Gollo et al., 2014; Palva and Palva, 2011). Accordingly, in-phase tACS aims to enhance synchronization and coordination between brain regions to improve specific cognitive functions, whereas out-of-phase tACS seeks to introduce interference or desynchronization to modulate cognitive processes (Alekseichuk et al., 2017; Polania et al., 2012; Reinhart, 2017; Tseng et al., 2018; Violante et al., 2017). However, the type of phase lag that can effectively enhance task performance and the underlying neurophysiological mechanisms remain controversial.

Therefore, in the present study, we investigated the neurodynamics associated with the phase-dependent neuromodulatory effects of tACS on inhibitory control using functional magnetic resonance imaging (fMRI) and functional connectivity analyses. We hypothesized that cognitive inhibitory processing is modulated by phase-dependent tACS between the L-dlPFC and the dACC. For this purpose, we administered individualized tACS with two different phase lags (0° or 180°) between two task-relevant key regions (i.e., the dlPFC and dACC) to participants while performing a color-word Stroop task.

2. Results

2.1. Behavioral data

Since a significant interaction effect between congruency and tACS-phase factors was observed in the reaction times normalized to the no-tACS condition ($F(2, 48) = 5.803$, $p < 0.05$), *post-hoc* tests were performed accordingly. Subsequent tests revealed that the 180°-phase-lag tACS yielded significantly reduced reaction times in the incongruent trials compared with the 0°-phase-lag tACS ($t(24) = 2.313$, $p < 0.05$, false discovery rate (FDR)-corrected; 180°-phase-lag tACS: 650.4 ms, 0°-phase-lag tACS: 677.7 ms: Fig. 1A). Trials with congruent conditions exhibited significantly reduced reaction times compared to trials with incongruent conditions for both 0°-phase-lag tACS ($t(24) = –6.295$, $p < 0.001$, FDR-corrected; congruent: 597.3 ms, incongruent: 677.7 ms) and 180°-phase-lag tACS ($t(24) = –5.713$, $p < 0.001$, FDR-corrected; congruent: 588.7 ms, incongruent: 650.4 ms). After the 0°-phase-lag tACS, the incongruent condition yielded significantly higher reaction times than the neutral condition ($t(24) = –4.678$, $p < 0.001$, FDR-corrected; incongruent: 677.7 ms, neutral: 568.0 ms). Regarding performance accuracy, a main effect of congruency was observed ($F(2, 48) = 14.950$, $p < 0.001$; congruent, 98.7 %,; incongruent, 96.2 %; neutral, 98.1 %). The other comparisons did not yield statistically significant results.

2.2. Brain activation during Stroop task performance

Random-effects group analyses of the phase-dependent tACS-induced blood oxygenation level-dependent (BOLD) responses revealed no significant difference in activation between 0°- and 180°-phase-lag tACS in both congruent and incongruent conditions. However, significantly greater activation was observed in the incongruent condition than in the congruent condition in the left putamen, dorsolateral prefrontal cortex (dlPFC), and primary motor cortex (M1) during 180° versus 0° phase-lag tACS (Fig. 2).

2.3. tACS-phase-dependent functional connectivity

During the Stroop task performance, functional connectivity was differentially modulated by the specific phase-lag tACS condition. Compared to the no-tACS and 0°-phase-lag tACS, the 180°-phase-lag tACS induced PFC-centered anterior-to-posterior connectivity (Fig. 3). In contrast, functional connectivity in the 0°-phase-lag tACS condition appeared to be randomly oriented compared to that in the 180°-phase-lag tACS-mediated well-oriented frontoparieto-occipital directions. Nevertheless, both 0°- and 180°-phase-lag tACS showed dominant connectivity based on the seed regions of the central executive network (CEN; pink regions in Fig. 3) when stronger connectivity was present in the congruent condition as opposed to the incongruent condition (blue arrows in Fig. 3). Conversely, dominant connectivity from the seed regions of the salience network (SN; green regions in Fig. 3) was observed when stronger connectivity occurred in the incongruent condition compared to the congruent condition (red arrows in Fig. 3). Regarding the default mode network (DMN), there were fewer modulations of functional connectivity from any seed regions, irrespective of the phase differences of the tACS signals. Particularly in the incongruent condition compared to the congruent condition (red arrows in Fig. 3), the left lateral geniculate nucleus (LGN) was a connectivity seed linked with the left pulvinar during the 180°-phase-lag tACS, whereas it was linked with the left/middle occipital cortex during the 0°-phase-lag tACS. In the context of the congruent condition compared to the incongruent condition (blue arrows in Fig. 3), the left LGN served as a connectivity seed linked with the right rostral PFC (a node of the SN) during the 180°-phase-lag tACS.

Between the tACS target regions (i.e., the dACC and left dlPFC), the differences in functional connectivity between the 0°- and 180°-phase-

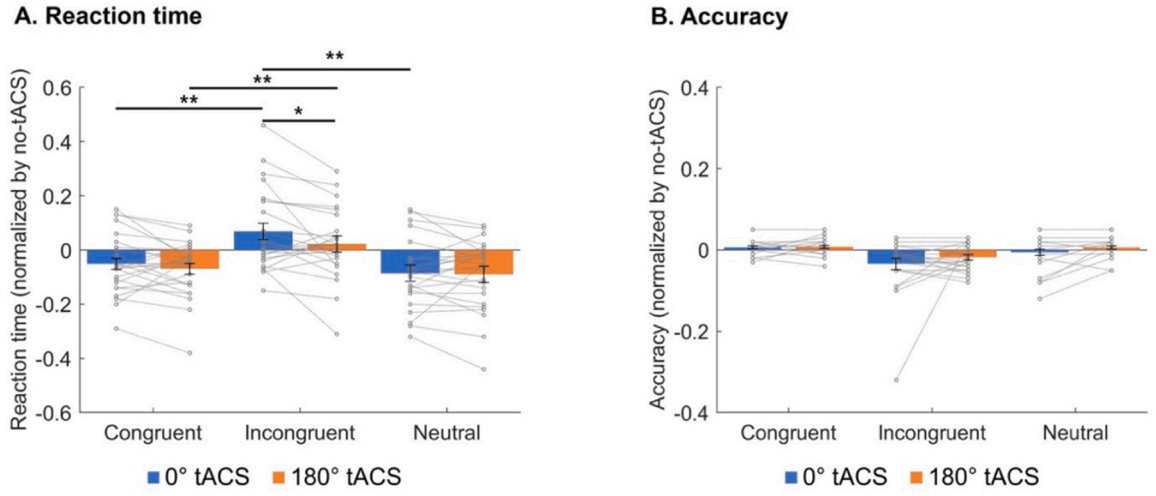

Fig. 1. Phase-dependent tACS-mediated changes in reaction times and accuracies. The 0°-phase-lag (blue bars) and 180°-phase-lag (orange bars) tACS-mediated mean (A) reaction times and (B) task performance accuracy, normalized by those in the no-tACS condition for the congruent, incongruent, and neutral conditions of the Stroop task. Small circles and their trajectories represent individuals' data and their tACS-mediated changes, respectively. Error bars indicate standard errors of the mean. Asterisks indicate statistical significance (*$p < 0.05$, ** $p < 0.001$, FDR-corrected).

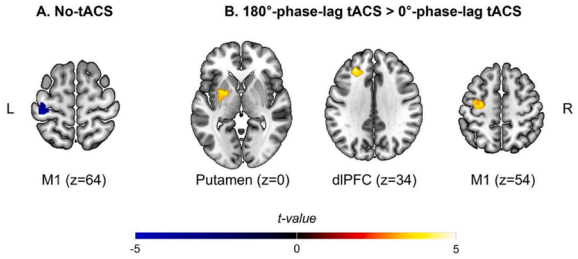

Fig. 2. 180°-phase-lag tACS-mediated brain activations in the incongruent condition. The significant activation regions for the (A) no-tACS and (B) 180°-phase lag tACS > 0°-phase-lag tACS conditions are displayed for the incongruent condition versus the congruent condition of the Stroop task (Incongruent > Congruent). As compared to the deactivation of the left primary motor cortex (M1) in the no-tACS condition, the left putamen, dorsolateral prefrontal cortex (dlPFC), and M1 were significantly more activated during the incongruent condition than in the congruent condition in the 180°-phase-lag tACS as compared to the 0°-phase-lag tACS (fMRI voxel-level threshold of $p < 0.001$ and a cluster-level family-wise error of $p < 0.05$). The positive t-values (in yellow) indicate activation, whereas the negative ones (in blue) indicate deactivation.

lag tACS conditions were marginally significant for the incongruent condition ($t(24) = 2.021$, $p = 0.055$, FDR-corrected), whereas the congruent condition was not statistically significant ($t(24) = 1.734$, *n.s.*, FDR-corrected). Compared to the no-tACS condition (z-score for no-tACS: 0.142), the congruent condition yielded significantly reduced functional connectivity between the dACC and left dlPFC by the 0°-phase-lag tACS ($t(24) = 5.322$, $p < 0.001$, FDR-corrected; z-score for 0°-phase-lag tACS: –0.108) and 180°-phase-lag tACS ($t(24) = 3.752$, $p < 0.01$, FDR-corrected; z-score for 180°-phase-lag tACS: –0.329). Similarly, compared to the no-tACS condition (z-score for no-tACS: 0.175), the incongruent condition showed significantly reduced functional connectivity between the dACC and left dlPFC for the 0°-phase-lag tACS ($t(24) = 2.719$, $p < 0.05$, FDR-corrected; z-score for 0°-phase-lag tACS: 0.051) and 180°-phase-lag tACS ($t(24) = 4.423$, $p < 0.01$, FDR-corrected; z-score for 180°-phase-lag tACS: –0.025).

In the incongruent condition, there were significant differences in functional connectivity related to the salience network between the two phase-lag tACS conditions (Fig. 4B). Compared to the no-tACS condition, the 0°-phase-lag tACS exhibited significantly enhanced functional connectivity between mediodorsal nucleus of the thalamus (MD) and rostral prefrontal cortex (rPFC) in the left hemisphere ($t(24) = –2885$, $p < 0.05$, FDR-corrected; z-score for no- tACS: –0.043, z-score for 0°-phase-lag tACS: 0.066) and significantly reduced functional connectivity between rPFC and supramarginal gyrus (SMG) in the right hemisphere ($t(24) = 3.063$, $p < 0.05$, FDR-corrected; z-score for no-tACS: 0.219, z-score for 0°-phase-lag tACS: 0.111). Compared to the no-tACS condition, the 180°-phase-lag tACS exhibited significantly enhanced functional connectivity between right dlPFC and left rPFC for both congruent ($t(24) = –4.141$, $p < 0.01$, FDR-corrected; z-score for no-tACS: 0.064, z-score for 180°-phase-lag tACS: 0.294) and incongruent conditions ($t(24) = –4.089$, $p < 0.01$, FDR-corrected; z-score for no-tACS: 0.104, z-score for 180°-phase-lag tACS: 0.304).

Furthermore, in the incongruent condition, compared to the 0°-phase-lag tACS, the 180°-phase-lag tACS exhibited significantly enhanced functional connectivity between rPFC and SMG in the right hemisphere ($t(24) = 5.537$, $p < 0.001$, FDR-corrected; z-score for 0°-phase-lag tACS: 0.111, z-score for 180°-phase-lag tACS: 0.301), and between right dlPFC and left rPFC ($t(24) = 4.972$, $p < 0.001$, FDR-corrected; z-score for 0°-phase-lag tACS: 0.097, z-score for 180°-phase-lag tACS: 0.304), while the opposite pattern was observed between MD and rPFC in the left hemisphere ($t(24) = –6.147$, $p < 0.001$, FDR-corrected; z-score for 0°-phase-lag tACS: 0.066, z-score for 180°-phase-lag tACS: –0.112). Among these brain regional pairs, the congruent condition yielded significant changes in functional connectivity only between the right dlPFC and left rPFC ($t(24) = 3.865$, $p < 0.01$, FDR-corrected; z-score for 0°-phase-lag tACS: 0.151, z-score for 180°-phase-lag tACS: 0.294; Fig. 4A).

2.4. Congruency-dependent functional connectivity

Compared with the functional connectivity of the congruent condition, the incongruent condition yielded further pruned and concentrated functional connectivity (Fig. 5). In particular, for the incongruent condition yielding a significant reduction in reaction times during the 180°-phase-lag versus the 0°-phase-lag tACS, strong functional connectivity was observed between the posterior cingulate cortex (PCC) and MD for the 180°-phase-lag tACS and between the ventrolateral prefrontal cortex (vlPFC) and fusiform gyrus (FUS) for the 0°-phase-lag tACS in the left hemisphere.

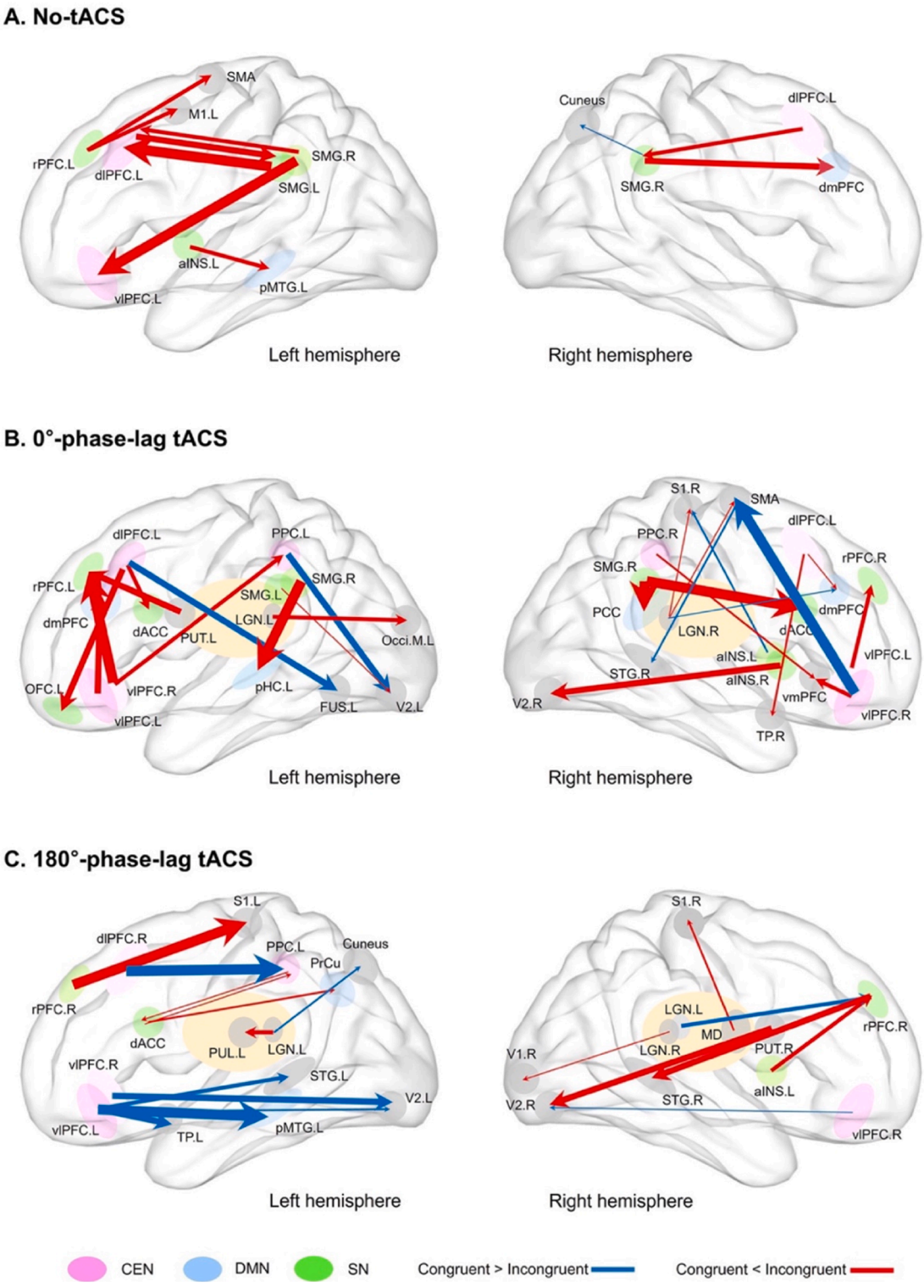

Fig. 3. tACS-phase-dependent functional connectivity. The (A) no-tACS, (B) 0°-phase-lag, and (C) 180°-phase-lag tACS-mediated functional connectivity. Only the statistically significant connectivity is displayed as arrows, and the thickness of the arrows represents *t* values ranging from 4.77 to 9.46. The starting points are the seeds for functional connectivity. The blue arrows indicate the cases when the congruent condition yielded higher connectivity than the incongruent condition, whereas the red arrows indicate the cases when the incongruent condition yielded higher connectivity than the congruent condition. The nodes of the central executive network (CEN), default mode network (DMN), and salience network (SN) are colored in pink, cyan, and green, respectively. aINS, anterior insula; dACC, dorsal anterior cingulate cortex; dlPFC, dorsolateral prefrontal cortex; dmPFC, dorsomedial prefrontal cortex; FUS, fusiform gyrus; LGN, lateral geniculate nucleus; M1, primary motor cortex; MD, mediodorsal nucleus of thalamus; Occi, occipital cortex; OFC, orbitofrontal cortex; PCC, posterior cingulate cortex; pHC, parahippocampal gyrus; pMTG, posterior middle temporal gyrus; PPC, posterior parietal cortex; PrCu, precuneus; PUL, pulvinar; PUT, putamen; rPFC, rostral prefrontal cortex; S1, primary somatosensory cortex; SMA, supplementary motor cortex; SMG, supramarginal gyrus; STG, superior temporal gyrus; TP, temporal pole; V1, primary visual cortex; V2, secondary visual cortex; vlPFC, ventrolateral prefrontal cortex; vmPFC, ventromedial prefrontal cortex; R, right; M, middle; L, left.

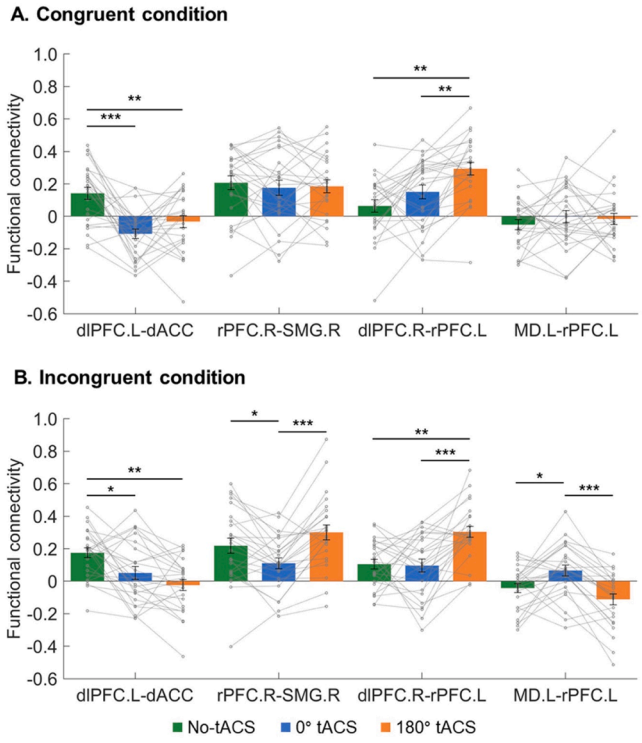

Fig. 4. Phase-dependent tACS-mediated changes in functional connectivity of the salience network. The mean z-scores of the functional connectivity across the nodes of the salience network are compared across no-tACS (green bars), 0° (blue bars) and 180°-phase-lag (orange bars) tACS in the (A) congruent and (B) incongruent conditions. Asterisks indicate statistical significance (* $p < 0.05$, ** $p < 0.01$, *** $p < 0.001$, FDR-corrected). Small circles and their trajectories represent individuals' data and their tACS-mediated changes, respectively. Error bars indicate standard errors of the mean. dACC, dorsal anterior cingulate cortex; dlPFC, dorsolateral prefrontal cortex; MD, mediodorsal nucleus of thalamus; rPFC, rostral prefrontal cortex; SMG, supramarginal gyrus; R, right; L, left.

2.5. Brain activation depends on the preceding congruency condition

Only in cases where the incongruent trials were preceded by incongruent trials (i.e., I-I condition), the 180°-phase-lag tACS yielded significantly reduced no-tACS-normalized reaction times compared to the 0°-phase-lag tACS ($t(24) = 2.791$, $p < 0.05$ FDR-corrected; 180°-phase-lag tACS: 643.6 ms, 0°-phase-lag tACS: 689.0 ms; Fig. 6A). No significant differences in reaction times were detected for other congruency combinations in consecutive trials. The accuracy of the task performance, depending on the preceding congruency condition, did not reach the statistical significance.

Regarding brain activation, similarly, only when incongruent trials were preceded by the incongruent trials (i.e., I-I condition), the 180°-phase-lag tACS induced significantly increased activation in the left putamen and left SMG compared with the 0°-phase-lag tACS (Fig. 6B). For any trial types preceded by the congruent trials (i.e., C-C, N-C, or I-C conditions), there were no statistically significant tACS-induced BOLD response modulations.

3. Discussion

This study investigated the effects of phase-manipulated tACS on brain activation and functional connectivity during an inhibitory control task. We observed a better task performance in the 180°-phase-lag tACS condition than in the 0°-phase-lag tACS condition (Fig. 1A). Notably, the 180°-phase-lag tACS induced significantly enhanced activation in the left putamen, dorsolateral prefrontal cortex, and primary motor cortex, particularly in the incongruent trials (Fig. 2). Subsequent tests revealed that this effect was prominent, particularly when incongruent trials were preceded by incongruent ones (Fig. 6). Furthermore, the 180°-phase-lag tACS yielded reinforced anterior-to-posterior functional connectivity compared to the 0°-phase-lag tACS and no-tACS treatments (Fig. 3). All these findings suggest that a specific phase of the two tACS signals targeting the two key functional nodes (i.e., the L-dlPFC and dACC) during the Stroop task is crucial for effective neuromodulations of inhibitory control.

3.1. 180°-phase-lag tACS-mediated enhanced activation in the putamen, dlPFC, and M1

We observed significantly enhanced brain activity in the putamen in the incongruent trials compared to the congruent trials during the 180°-phase-lag tACS condition compared to the 0°-phase-lag tACS condition. Moreover, this 180°-phase-lag tACS-induced behavioral improvement and putamen activation were consistently observed only in incongruent trials preceded by incongruent trials (Fig. 6B). The putamen plays an essential role in various movement-related functions (Alexander and Crutcher, 1990; Marchand et al., 2008). Previous studies have shown that the putamen is not functionally limited to motor control tasks, and reflects the interaction between memory, action, and rewards (Koster et al., 2015; Voytek and Knight, 2010). The putamen is also associated with cognitive processes such as cognitive control (Salvia et al., 2019; Swick et al., 2011). The cognitive inhibitory function of the putamen is not as extensively studied or well-defined as its motor-related function; however, several studies have suggested that the putamen may play a modulatory role in cognitive functions, including cognitive inhibition (Aizenstein et al., 2006; Monchi et al., 2006). Presumably, consecutive incongruency (i.e., incongruent trials preceded by incongruent trials) might induce reinforced activation of the putamen, reflecting accumulated cognitive inhibition, which might be influenced by the 180°-phase-lag tACS, resulting in reduced reaction times in the Stroop task (Fig. 6).

The predominant functions of cognitive control are response selection and inhibition (Goghari and MacDonald III, 2009). Previous studies have identified brain regions involved in inhibition, including the basal ganglia (such as the putamen), which are thought to be involved in the inhibition of inappropriate responses, and prefrontal regions (such as the dlPFC), which receive inputs from the basal ganglia thalamocortical circuit and represent and maintain relevant information for goal-directed behaviors (Aron et al., 2014; Booth et al., 2003; Casey et al., 2001; Maciejewski et al., 2018). Consistently, the left dlPFC, the target region of tACS, was activated under the same conditions (Fig. 2). It is implicated in the suppression of irrelevant or inappropriate responses, cooperatively allowing for the selection and execution of the most appropriate actions based on the current goals and contexts. Consequently, we observed that the 180°-phase-lag tACS induced both enhanced putamen activation and dlPFC-mediated top-down inhibitory control.

We also observed enhanced activation in the primary motor cortex (M1) in incongruent trials of the 180°-phase-lag tACS versus the 0°-phase-lag tACS. The putamen and M1 are two distinct brain regions that play pivotal roles in inhibitory functions, including cognitive and motor inhibition (Guo et al., 2018). Although both the putamen and M1 contribute to inhibitory functions in the context of motor control, the M1 is more directly involved in motor execution and precision, while the putamen, as part of the basal ganglia, plays a broader role in motor planning and regulation (Bhattacharjee et al., 2021; Guo et al., 2018). Aspects of cognitive inhibition are more indirect and complicated, with the M1 playing a contributing role, especially in coordination with other cortical regions (Fujiyama et al., 2016). The M1 may play a tactical role in inhibiting competing motor plans or adjusting movements based on cognitive demands. Taken together, the facilitation of cognitive and motor inhibitory control might result in significantly reduced reaction

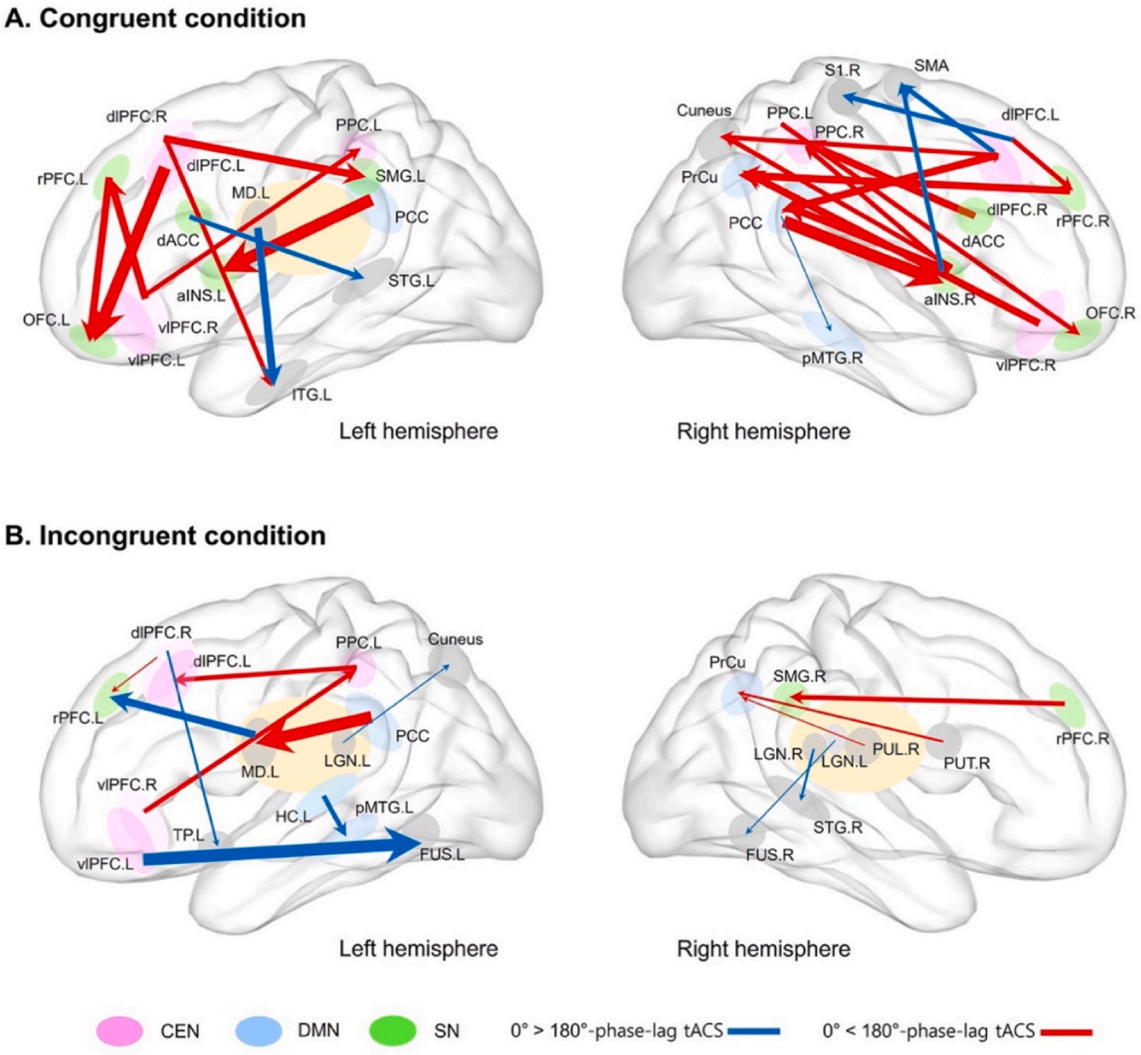

Fig. 5. Congruency-dependent functional connectivity. Both 0°- and 180°-phase-lag tACS-mediated functional connectivity are shown in the (A) congruent and (B) incongruent conditions of the Stroop task. Only the statistically significant connectivity is displayed as arrows, and the thickness of the arrows represents *t* values ranging from 4.77 to 9.46. The starting points are the seeds for functional connectivity. The blue arrows indicate the cases when the 0°-phase-lag tACS yielded higher connectivity than the 180°-phase-lag tACS, whereas the red arrows indicate the cases when the 180°-phase-lag tACS yielded higher connectivity than the 0°-phase-lag tACS. The nodes of the central executive network (CEN), default mode network (DMN), and salience network (SN) are colored in pink, cyan, and green, respectively. aINS, anterior insula; dACC, dorsal anterior cingulate cortex; dlPFC, dorsolateral prefrontal cortex; FUS, fusiform gyrus; HC, hippocampal gyrus; ITG, inferior temporal gyrus; LGN, lateral geniculate nucleus; MD, mediodorsal nucleus of thalamus; OFC, orbitofrontal cortex; PCC, posterior cingulate cortex; pMTG, posterior middle temporal gyrus; PPC, posterior parietal cortex; PrCu, precuneus; PUL, pulvinar; PUT, putamen; rPFC, rostral prefrontal cortex; S1, primary somatosensory cortex; SMA, supplementary motor cortex; SMG, supramarginal gyrus; STG, superior temporal gyrus; TP, temporal pole; vlPFC, ventrolateral prefrontal cortex; R, right; M, middle; L, left.

times for incongruent trials during the 180°-phase-lag tACS versus the 0°-phase-lag tACS. Since all participants in the present study were right-handed, left-lateralized activation in the putamen, dlPFC, and M1 appeared to be observed.

3.2. 180°-phase-lag tACS-mediated anterior-to-posterior top-down control

Compared with the 0°-phase-lag tACS condition, the 180°-phase-lag tACS condition yielded prominent anterior-to-posterior functional connectivity (Fig. 3C). Functional connectivity in the 0°-phase-lag tACS condition appeared randomly oriented compared to that in the 180°-phase-lag tACS-mediated well-oriented frontoparieto-occipital directions. When the functional connectivity of the two tACS target regions was compared, the 0°-phase-lag tACS revealed a marginally significant enhancement in the incongruent condition compared to the congruent condition. Such congruency-dependent modulation by phase-dependent tACS may imply to consider task-dependent and regional-distance-dependent neuromodulatory dynamics when interpreting the observations although previous studies have reported the principal relationship between in-phase electrical stimulation and optimal behavioral performance (Alekseichuk et al., 2017; Polanía et al., 2014, 2015; Polania et al., 2012; Reinhart, 2017; Tseng et al., 2018; Violante et al., 2017) or synchronization of oscillatory activity in the stimulated brain regions as its neurophysiological basis (Helfrich et al., 2014; Huang et al., 2021; Wischnewski et al., 2024). Presumably, the 0°-phase-lag tACS may facilitate local cortico-cortical networking within a short-time scale, while the 180°-phase-lag tACS may involve long-range communication (Alekseichuk et al., 2019) or inhibitory top-down control as shown in the incongruent condition of this study. Within the 180°-phase-lag tACS-mediated anterior-to-posterior long-range functional connectivity, the PFC seemed to functionally

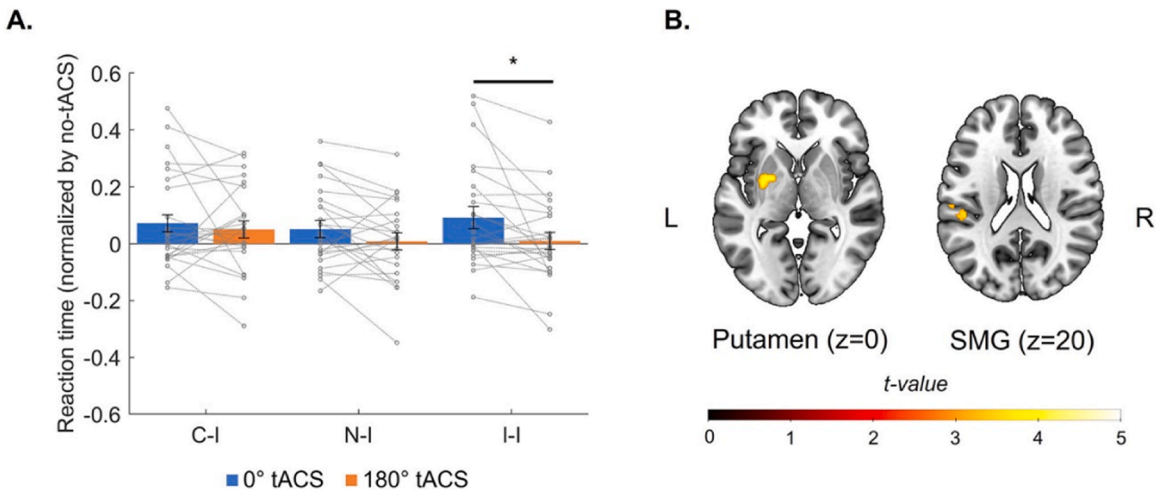

Fig. 6. Behavioral performance and brain activation for incongruent trials preceded by the incongruent trials. (A) In cases where the incongruent trials were preceded by the incongruent trials (i.e., the I-I condition), the 180°-phase-lag tACS yielded significantly reduced reaction times than the 0°-phase-lag tACS (* $p <$ 0.05, FDR-corrected). Reaction times are normalized with the no-tACS condition. Small circles and their trajectories represent individuals' data and their tACS-mediated changes, respectively. Error bars indicate standard errors of the mean. C-I, congruent-incongruent trial-pair condition; N-I, neutral-incongruent trial-pair condition; I-I, incongruent-incongruent trial-pair condition. (B) For this I-I condition, the left putamen and the left supramarginal gyrus (SMG) exhibited significantly enhanced activation for the 180° phase-lag tACS versus the 0° phase-lag tACS.

influence the posterior cortical regions in a top-down manner. As the PFC is one of the core regions of the CEN, its fundamental functions are associated with executive functions, attentional control, and working memory, including goal-directed behavior (Fuster, 2001). Increased connectivity within the CEN may be expected during tACS because this network is implicated in cognitive control processes associated with the dlPFC. Previous studies have suggested that tACS administered to the dlPFC can enhance the functional connectivity between the dlPFC and other brain regions, including the ACC (Khan et al., 2023; Lehr et al., 2019). This heightened connectivity is thought to modulate cognitive processes related to attention, working memory, and decision-making.

As depicted in Fig. 7, it is widely accepted that the coordination of mutually antagonistic CEN and DMN plays a key regulatory role in organizing the neural responses underlying fundamental brain functions (Nekovarova et al., 2014). The anti-correlated relationship between the CEN and DMN during most cognitive functions has been well established (Menon, 2011; Sridharan et al., 2008). For instance, during the performance of cognitively demanding tasks, cognitive states that activate the CEN typically deactivate the DMN, and vice versa (Fox et al., 2006; Greicius et al., 2003; Raichle et al., 2001a). Notably, the tACS-induced

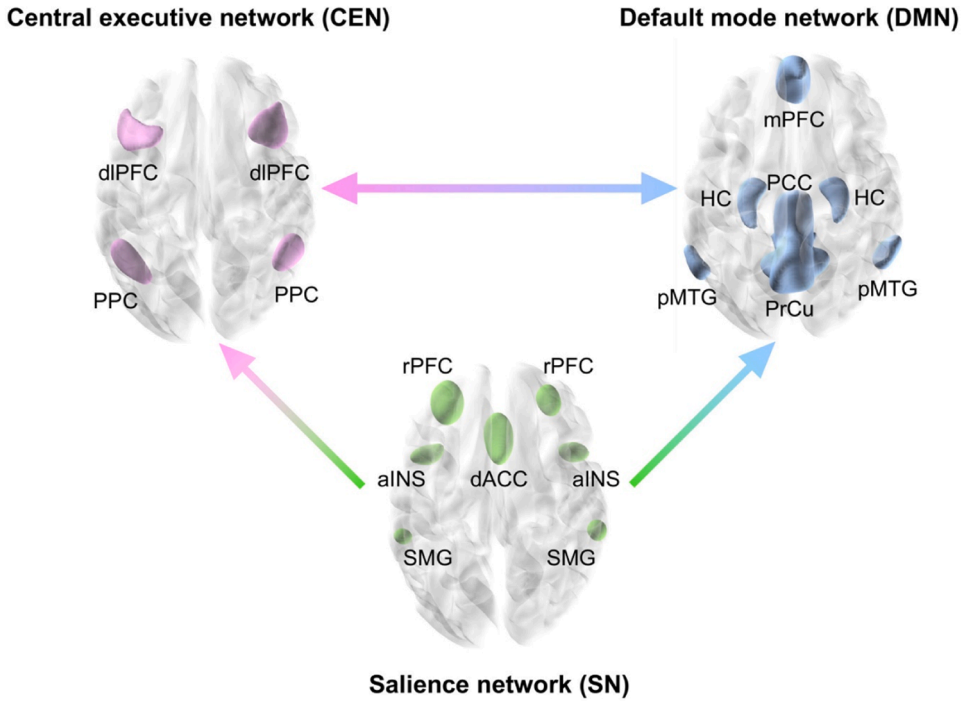

Fig. 7. Anti-correlated brain network model. The anti-correlated relationship between the central executive network (CEN; pink regions) and default mode network (DMN; cyan regions), which are regulated by the salience network (SN; green regions). aINS, anterior insula; dACC, dorsal anterior cingulate cortex; dlPFC, dorsolateral prefrontal cortex; HC, hippocampus; mPFC, medial prefrontal cortex; PCC, posterior cingulate cortex; pMTG, posterior middle temporal gyrus; PPC, posterior parietal cortex; PrCu, precuneus; rPFC, rostral prefrontal cortex; SMG, supramarginal gyrus.

neuromodulation of functional connectivity was observed in the SN, including the insula and dACC (Fig. 3). As tACS-mediated dominant functional connectivity in the incongruent condition was observed in the seed regions of the SN (green regions in Fig. 3), the SN appeared to play an essential role in the inhibitory control of the incongruent condition. Consistent with this, the functional connectivity within the SN was significantly more modulated by phase-dependent tACS in the incongruent condition than in the congruent condition (Fig. 4). The dynamics of switching between the anti-correlated CEN and DMN are controlled by the SN, which is involved in recruiting relevant functional networks (Menon and Uddin, 2010; Peters et al., 2016; Sridharan et al., 2008). Indeed, the insula is known as a multimodal integration region providing an interface between external information and internal motivational states (Craig, 2009; Seeley et al., 2007). For instance, the anterior insula is involved in a wide range of cognitive processes, including switching between cognitive resources (Uddin and Menon, 2009) and reorienting attention (Ullsperger et al., 2010). The dorsal anterior insula and dACC are functionally connected to a set of regions described as cognitive control networks (Dosenbach et al., 2007; Grinband et al., 2006). Compared to the posterior insula, it has been suggested that the anti-correlation pattern between the CEN and DMN is modulated by an anterior insula-based network, primarily comprising the anterior insula and dACC (Chand and Dhamala, 2016; Sridharan et al., 2008). Thus, the insula has been consistently implicated in switching the dominant processing network between the CEN and the DMN, serving as one of the key nodes in the SN.

Additionally, tACS-mediated functional connectivity was observed in the dACC, another key node in the SN. The dACC is associated with attentional processes, including error detection, conflict monitoring, and performance evaluation (Botvinick et al., 2001; Bush et al., 2000; Shenhav et al., 2013). Activity in this region closely mirrors the level of control recruited in conflict scenarios and has a strong functional relationship with the lateral PFC (Botvinick, 2007; Botvinick et al., 2004; Kerns et al., 2004). This notion can be expanded to incorporate a conflict monitoring unit represented by the dACC, which signals the level of control required to facilitate processing in the task-relevant pathway implemented by the dlPFC (Botvinick et al., 2001; Krug and Carter, 2012). Moreover, the time course of activity in the dlPFC and dACC during top-down attentional control reveals a dynamic interplay between these regions in orchestrating cognitive processes related to attention regulation (Banich, 2019; Silton et al., 2010). Considering the dynamic interactions in activation between the L-dlPFC and dACC, especially with the 180°-phase-lag tACS, it seems that this condition was more effective, particularly for the incongruent condition, in inducing better behavioral performance compared with the condition without considering the temporal difference in the 0°-phase-lag tACS. It is likely that the different phase lags simulate temporally delayed stimulation between the L-dlPFC and the dACC. Recent models further explored and tested the temporal dynamics between these two regions (Banich, 2009, 2019; Oehrn et al., 2014; Silton et al., 2010).

While only the left parahippocampal gyrus (the primary hub of the DMN during the resting state (Ward et al., 2014)) was notably associated with the SMG (a node of the SN), specially in the incongruent condition during the 0°-phase-lag versus 180°-phase-lag tACS, the DMN exhibited comparatively lower functional connectivity compared to the CEN and SN. Presumably, as the present study applied phase-lagged tACS to the L-dlPFC (a node of the CEN) and the dACC (a node of the SN), tACS-mediated modulation of functional connectivity was observed in both the CEN and SN, but not in the DMN. Additionally, the DMN is predominantly active during rest and is often associated with internally focused and self-referential processes (Raichle et al., 2001b; Sormaz et al., 2018). Thus, the inhibitory-controlled feature processing of externally presented colored words in the Stroop task might not involve functional connectivity in the DMN.

The thalamus is also known to regulate conscious perception through inhibitory control within the thalamocortical network (Halassa and Acsády, 2016; Min et al., 2020; Seo et al., 2022). Consistently, regarding the tACS-mediated subthalamic connectivity in the present study, it is noteworthy that the functional connectivity between the pulvinar and LGN was enhanced in the incongruent condition during the 180°-phase-lag tACS. As the pulvinar is also crucially involved in cognitive control (Halassa and Kastner, 2017; Michael and Buron, 2005; Phillips et al., 2021), this observation corroborates the 180°-phase-lag tACS-mediated facilitation of inhibitory control, particularly in the incongruent condition.

However, the present study has several limitations. First, owing to current technical limitations, deep brain structures, such as the dACC, were not efficiently stimulated using the scalp-based tACS device (Fig. 8E). In the present study, the stimulation power of the target areas was also limited by individuals' sensation thresholds of the input current. Moreover, since the averaged simulation electric field in this study (0.12 V/m) was below the minimum of 0.2 V/m to modulate neurons in awake and behaving mammals (Alekseichuk et al., 2022; Reato et al., 2010), a more enhanced stimulation intensity would have improved the observed neuromodulatory effect for future research. A recent neuromodulatory approach using temporal interference has begun to elucidate a non-invasive way to selectively stimulate deep-brain structures (Esmaeilpour et al., 2021; Grossman et al., 2017), which may provide further corroborating evidence for future studies. Second, the EEG theta frequency should be computed under the no-tACS condition for the subsequent tACS resonating frequency, and the long experimental time (when including both no-tACS and sham conditions) could induce fatigue in participants leading to poor data quality; therefore, the present study employed only the no-tACS condition instead of the tACS-sham condition. Thus, the present study focused on the tACS phase-dependent modulatory effect between in-phase (0°) and out-of-phase (180°) lags across the dlPFC and dACC on subsequent behavioral and neurodynamic changes. Third, the effects of tACS are known to be mediated by retinal (Schutter, 2016) and somatosensory (Asamoah et al., 2019) stimulation, which should be carefully considered when interpreting our observations in cortical regions.

In conclusion, our observations provide convincing evidence that a specific phase-lag tACS between two essential nodes effectively modulates relevant cognitive functions, thereby facilitating inhibitory control. Our findings suggest that at least some of the variability in non-invasive brain stimulation effects may be attributed to stimulation-signal phase relationships across task-relevant brain networks, indicating that this point should be considered when designing a neuromodulatory paradigm. The potential applications of specific-phase-lag tACS are manifold, ranging from therapeutic perspectives in cognitive rehabilitation to cognitive augmentation, such as attention deficit/hyperactivity disorder (ADHD). By individually refining the optimal phase-lag tACS configurations and revealing their neurophysiological underpinnings, precise and robust neuromodulation can be achieved for a wide range of neuromodulatory applications.

4. Material and methods

4.1. Participants

Thirty-one healthy volunteers (13 females; mean age 23.6 ± 3.2 years) participated in this study. All the participants had normal or corrected-to-normal vision. None of the participants had a history of psychiatric or neurological disorders, contra-indications for MRI scanning, current and past alcohol/drug abuse or dependence, or current use of illicit substances. This study was conducted in accordance with the ethical guidelines of the Institutional Review Board of the Korea University (No. KUIRB-2021–0209–08). All participants provided written informed consent.

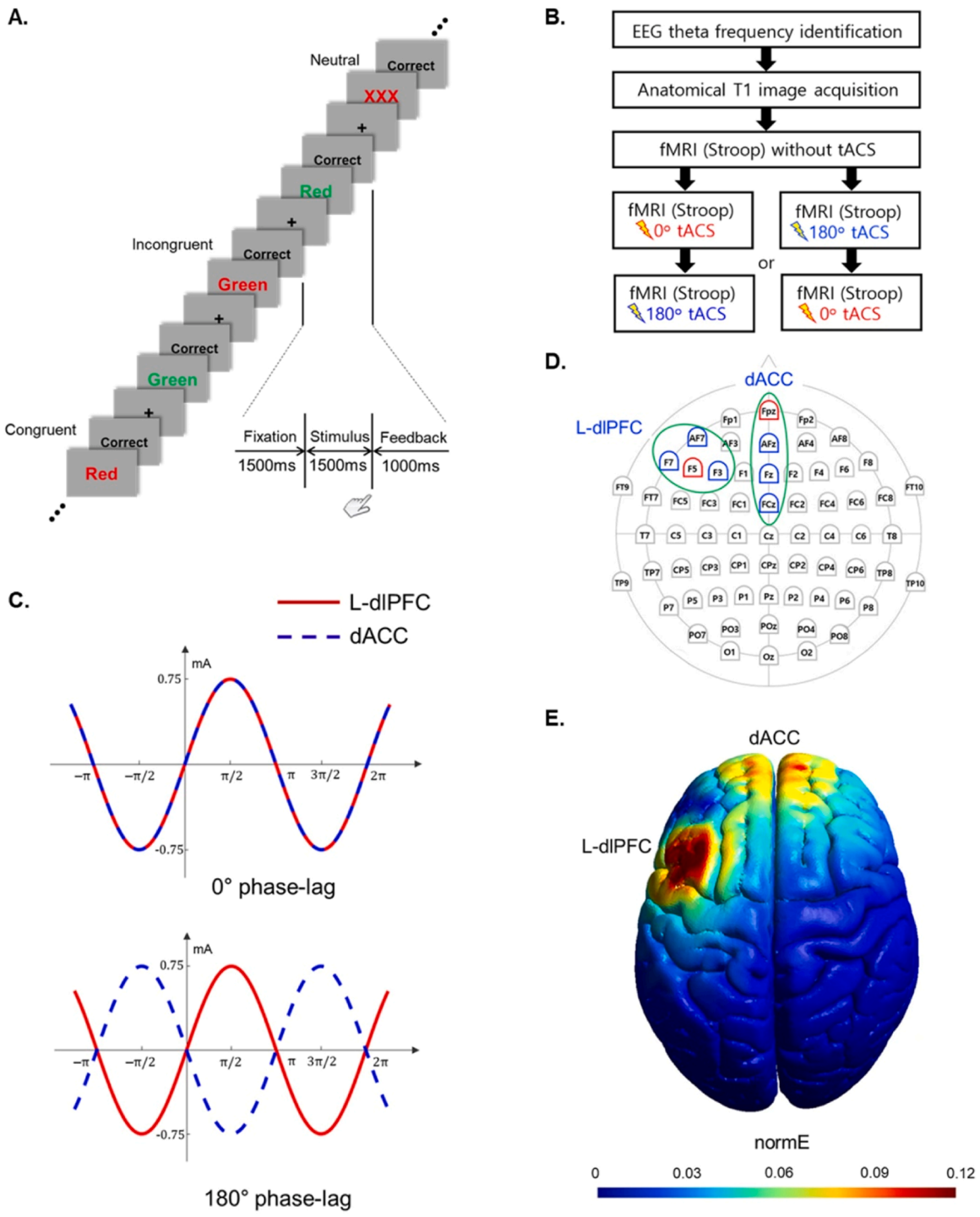

Fig. 8. Experimental design: Stroop task and tACS simulation with a phase lag. (A) We used a color naming Stroop task. The two color-word stimuli employed were the words "Red" and "Green", presented either in red or green hue on a gray background. Stimuli were presented for 1500 ms with an inter-stimulus interval (ISI) of 1500 ms. Participants were instructed to respond as fast as possible by pressing buttons indicating whether the stimulus word matched its color and naming. Visual feedback was provided immediately after each response. (B) Before the main experiment, individual tACS theta frequencies were identified using EEG data during the Stroop task performance without tACS, and anatomical T1 images were obtained for the subsequent tACS treatment. The Stroop task was repeatedly applied to the same participant before and during either the 0°-phase-lag or 180°-phase-lag tACS. The order of 0°- and 180°-phase-lag tACS sessions was counterbalanced across participants, and tACS was applied for the entire period of the Stroop task. (C) tACS stimulation waveforms in the L-dlPFC (red solid line) and dACC (blue dashed line) with 0°-phase-lag (upper panel) or 180°-phase-lag (lower panel) tACS. (D) tACS channel montage for a sample participant. The red color indicates stimulation channels, and the blue color represents surrounding return channels. Each green ring indicates a modular subset of stimulation and return channels for each target region. L-dlPFC, left dorsolateral prefrontal cortex; dACC, dorsal anterior cingulate cortex. (E) Simulation of the tACS-induced electric field in the L-dlPFC and dACC. The unit *normE* denotes the normalized strength of the induced electric field (V/m), with high intensities indicated in red and low intensities represented in blue.

4.2. Task paradigm

We used the color-word Stroop task (Stroop, 1935) to assess for inhibitory control (Fig. 8A). The Stroop task is appropriate for studying the neurodynamics related to cognitive control as it requires attentional allocation and inhibitory processes with conflicting features. Task stimuli consisted of congruent, neutral, and incongruent conditions. The stimuli were colored words ("Red" and "Green") written in congruent or incongruent colors, while neutral stimuli were meaningless streams of letters ("XXX"). The items were presented randomly and equally to each participant using presentation software (E-prime 3.0 Professional, Psychology Software Tools Inc., Sharpsburg, USA).

The participants were instructed to respond as quickly as possible by pressing a button with their right or left index finger indicating the color of the presented letter stimulus. The response hands were counterbalanced across participants. Afterward, visual feedback in the form of "Correct," "Incorrect," or "No Response" was displayed to motivate participants to perform the task better. The inter-trial interval was 1500 ms, during which a fixation cross was presented at the center of the screen. Each participant completed three task sessions, each comprising 45 trials per congruency condition (i.e., congruent, incongruent, and neutral conditions) for a total of 135 trials per task session.

4.3. Individual theta-frequency tACS neuromodulation

Before the main experiment, we conducted fMRI to localize the brain regions activated during the Stroop task and to optimize the stimulation electrode placement. We used the initial fMRI data from the Stroop task without tACS to individually identify the target regions, specifically the L-dlPFC and the dACC. Electrode placement was then planned to maximize the tACS-induced electric field intensity in the target regions. Electrode-placement optimization was performed using SimNIBS (ver. 3.2.6, DRCMR & DTU, Denmark) (Thielscher et al., 2015) and tES LAB (ver. 3.0, Neurophet, Seoul, Korea) simulation software. For spatially accurate stimulation, the participant-specific optimized coordinates of the target regions for stimulation were computed based on individual T1 images obtained before the main experiment (Fig. 8B). Electrode placements were selected to optimize the strength of the electric field at the target locations. The optimal stimulation power was determined based on the attainment of maximum intensity in both the two target regions (i.e., the L-dlPFC and dACC) when manipulating the combination of input/return-electrode positions around the scalp target regions using individual sensation thresholds of the input current. For each target region, we selected one stimulation electrode (marked in red) and three return electrodes (marked in blue; sample channel-montage, Fig. 8D). The currents of all stimulation and return channels were configured to maintain the total current at zero. Using tES LAB simulation software, we examined whether the stimulation signals matched the intended phase lag (either 0° or 180°) before the main study. Utilizing an oscilloscope, we double-checked whether the phase-lag manipulated signals physically generated the exact amplitude, shape, and frequency intended for the design phase. The averaged simulation electric-field intensity was 0.12 V/m (standard deviation: 0.02 V/m) at the activated cortical region. As shown in Fig. 8E, the simulation results demonstrated that the activation regions were well aligned with the intended target regions.

The choice of theta frequency (ranging from 4 to 8 Hz and individually obtained by each participant) for tACS signals between the L-dlPFC and dACC was based on the stronger connectivity observed in these regions during conflict situations, such as incongruent conditions in the Stroop task, particularly in the electroencephalographic (EEG) theta band (Cohen and Cavanagh, 2011; Hanslmayr et al., 2008; Nigbur et al., 2012; Oehrn et al., 2014). The neuromodulatory effect is maximized when the stimulus wave (i.e., tACS) closely resembles the target wave (i.e., the human brain wave), thus supporting the selection of the theta frequency for the tACS signals in the present study. Differentiation between congruent and incongruent conditions has consistently been observed in temporal neurodynamic patterns in the left dlPFC, followed by dACC activation (Silton et al., 2010). Furthermore, the application of anodal tDCS to the left dlPFC led to improved behavioral responses during Stroop task performance (Angius et al., 2019; Loftus et al., 2015).

Individual theta frequencies were determined individually for every participant, as the dominant theta peak frequency during the Stroop task performance varied between the participants. The theta frequencies (4–8 Hz) for each participant were individually determined based on the EEG data of the Stroop task without tACS treatment before the main fMRI experiment and were administered as personalized theta-frequency sinusoidal tACS signals. This approach is based on the close relationship between the midfrontal theta frequency band during conflict situations and central executive function (Cavanagh and Frank, 2014; Cohen and Donner, 2013). To individually determine midfrontal theta peak frequencies before the main tACS experiment (Fig. 8B), using the fast Fourier transform, the frequency (ranging from 4 to 8 Hz) was chosen when its maximum power at the midfrontal electrodes Fz, F1, and F2 was detected within the time window between stimulus onset and 1 s poststimulus during the no-tACS Stroop task (mean theta peak frequency with its standard deviation: 5.68 ± 1.41 Hz). EEG signals were recorded using a BrainAmp DC amplifier (Brain Products, Germany) with 64 Ag/AgCl electrodes, according to the international 10–10 system. A reference electrode was placed at the tip of the nose and the AFz electrode was used as the ground electrode. Electrode input impedances were kept below 10 kΩ prior to the data acquisition. EEG data were collected at a sampling frequency of 500 Hz using a high-pass filter (cut-off frequency: 0.5 Hz) with a notch filter of 60 Hz. To determine individual theta frequencies, EEG data were epoched from stimulus onset to 1000 ms poststimulus. Eye movement activity was monitored with an EOG electrode placed sub-orbitally to the left eye, and vertical and horizontal electro-ocular activity was computed using two pairs of electrodes placed vertically and horizontally with respect to both eyes (i.e., Fp1 and EOG for the vertical EOG; F7 and F8 for the horizontal EOG). All epochs were visually inspected for artifacts, and epochs containing eye movements or other artifacts (maximum amplitude ±100 μV and maximal gradient voltage step 50 μV/ms) were automatically rejected from further analyses. Only the trials with correct responses were collected for further analysis.

Phase-modulated tACS was delivered online for the entire duration (9 min) of the Stroop task using an MR-compatible $M \times N$ 65 high-definition (HD) transcranial electrical stimulator (tES) system (Soterix Medical Inc., New York, USA). The tACS intensities were kept below individual sensation thresholds, using the task-relevant frequency within the theta band. The peak-to-peak amplitude ranged from 0.3 to 1.5 mA, tailored for each participant.

4.4. Experimental procedure

Stimulation of the L-dlPFC and dACC was performed with either a 0°- or 180°-phase-lag. Among the tACS phase-lag values that may induce efficient facilitation or suppression of task performance, we selected in-phase (0°) and out-of-phase (180°) lags for the present study. This choice was based on previous studies that empirically reported optimal behavioral performance when the DMN led the CEN with a full or partial phase lag, and a 180°-phase-lag (full anti-phase) resulted in the least favorable behavioral performance during cognitive tasks (Alekseichuk et al., 2017; Polanía et al., 2014, 2015; Polania et al., 2012; Reinhart, 2017; Tseng et al., 2018; Violante et al., 2017).

The Stroop task was repeatedly applied to the same participant before and during either the 0°-phase-lag or 180°-phase-lag tACS to investigate the ongoing effects of phase-lag-modulated tACS treatment on inhibitory control. Each experiment consisted of three 9-min-long sessions, between which short breaks were given (Fig. 8B). We conducted two tACS-treatment sessions, during which tACS was administered for 9 min (with 30-s ramp-up and ramp-down periods) with either

a 0° (in-phase) or 180° (out-of-phase) phase difference between the L-dlPFC and dACC (Fig. 8C). The task flow was as follows: (1) fMRI-session performing the task without tACS; (2) tACS-fMRI session performing the task with a 0°-phase-lag tACS; and (3) tACS-fMRI session performing the task with a 180°-phase-lag tACS (Fig. 8B). The order of the 0° and 180° phase-lag tACS sessions was counterbalanced across participants. Participants were debriefed immediately after the last session. During the debriefing, the participants indicated their subjective perception (or any uncomfortable experience, including retinal phosphenes) of the stimulation. We analyzed both reaction times and accuracy as behavioral measures of task performance. Each participant's reaction times were fitted to a gamma distribution and collected within a 95 % confidence interval (De Boeck and Jeon, 2019). To control for inter-individual variability in behavioral performance, the post-treatment values for both reaction times and accuracies were individually normalized by their pre-treatment values in the no-tACS condition. Normalized reaction times and performance accuracies were compared using repeated-measures ANOVA with a tACS phase factor (no-tACS normalized 0°- and 180°-phase-lag behavioral results) and a congruency factor (congruent, incongruent, and neutral) of the Stroop task. If a significant interaction effect was detected, subsequent tests were conducted using FDR-corrected two-sided paired *t*-tests (Benjamini and Hochberg, 1995).

4.5. fMRI data acquisition

Whole-brain images were collected using a Siemens 3 Tesla MAGNETOM Trio Tim Syngo scanner (Siemens Healthcare, Erlangen, Germany) and a 32-channel head coil. Before the experiment, the participants received a detailed explanation of the experimental procedure and were familiarized with the experimental surroundings and stimuli. The participants were instructed to keep their eyes open and gaze at the MR-compatible screen located at the end of the MRI bed through a mirror positioned on the head coil. The distance between the screen and participants was approximately 245 cm, and the diameter of the stimulus on the screen was 30 cm, resulting in a visual angle of 7.0°. To maximize the participants' concentration in the task, darkness was maintained both inside and outside the MRI-shielding room during the experiment. After acquiring automated scout images and performing shimming procedures to optimize field homogeneity, 270 fMRI image volumes were collected using an interleaved T2*-weighted echo-planar imaging sequence for each fMRI session. A total of 75 slices per volume were obtained using the following parameters: repetition time (TR) = 2000 ms, echo time (TE) = 30 ms, flip angle (FA) = 90°, multiband acceleration factor = 3, acquisition matrix = 96 × 96, field of view = 192 × 192 mm^2, in-plane voxel size = 2 × 2 × 2 mm^3, and no slice gap. High-resolution structural scans of 3-dimensional anatomical magnetization prepared rapid acquisition gradient echo (MP-RAGE) images were collected for each participant after fMRI data collection (TR = 2.3 s, TE = 2.13 ms, inversion time = 0.9 s, FA = 9°, acquisition matrix = 256 × 256, in-plane voxel size = 1 × 1 × 1 mm^3, and 224 sagittal slices).

4.6. fMRI data analysis

BOLD images were processed and analyzed using Statistical Parametric Mapping (SPM12; https://www.fil.ion.ucl.ac.uk/spm/software/spm12) in MATLAB (ver. R2021a, MathWorks, Natick, USA). Functional images were preprocessed using a standard task-based fMRI processing pipeline: slice-timing correction (using the first slice as the reference slice), motion correction, co-registration, gray/white matter segmentation, normalization to the Montreal Neurological Institute template, and spatial smoothing using a 6-mm full-width at half-maximum Gaussian kernel. A temporal high-pass filter with a 128-s cutoff was applied to remove low-frequency signal drift, and serial correlations from aliased biorhythms in the time series were adjusted using an autoregressive AR 1 model (Bullmore et al., 1996). The movement parameters from the realignment procedure (x, y, z, roll, pitch, and yaw) were used as regressors of non-interest in the first-level analysis. Although the majority of participants exhibited minimal movement during the functional scan of each fMRI session (< 3 mm and 3° for all participants), data from six participants were excluded from further analyses because of excessive head motion.

In the first-level analysis, we examined whole-brain activity for each trial type (congruent, C; incongruent, I; and neutral, N) relative to a fixation block, as well as for their differences (e.g., congruent minus incongruent) for each fMRI session (no-tACS, 0°-phase-lag tACS, and 180°-phase-lag tACS). To investigate the effect of phase-dependent tACS treatment on inhibitory control, the generated contrast images (congruent > fixation, incongruent > fixation, neutral > fixation, and congruent > incongruent) for each fMRI session were submitted to a second-level analysis across participants, which employed a general linear model with random effects to identify the brain regions that averaged the within-tACS-condition using one-sample *t*-tests. We also submitted contrast maps to a flexible factorial design (analogous to a repeated-measures ANOVA) to assess possible interactions across the Stroop and phase-dependent tACS effects, including 3 (congruent, incongruent, and neutral conditions) × 3 (no-tACS, 0°-phase-lag tACS, and 180°-phase-lag tACS) factors. To correct for multiple comparisons, a voxel-level threshold of $p < 0.001$ and a cluster-level family-wise error (FWE) of $p < 0.05$ were used.

To subsequently evaluate the behavioral and neurodynamic modulation following tACS treatment, based on the preceding congruency type (congruent, neutral, and incongruent), we further analyzed the behavioral and fMRI data. Specifically, we explored the following pairs: congruent-congruent (C-C), neutral-congruent (N-C), incongruent-congruent (I-C), congruent-incongruent (C-I), neutral-incongruent (N-I) and incongruent-incongruent (I-I) pairs.

4.7. Functional connectivity analyses

To investigate the phase-lag tACS-mediated differences in functional connectivity between congruent and incongruent trials during the Stroop task, we conducted seed-based functional connectivity in both the 0°- and 180°-phase-lag tACS using the functional connectivity toolbox (CONN toolbox, ver. 20b; https://www.nitrc.org/projects/conn/) (Whitfield-Gabrieli and Nieto-Castanon, 2012). To define task-relevant regions of interest (ROIs), we employed the default atlas in the CONN toolbox. This atlas integrates the CONN's human connectome project independent component analysis (HCP-ICA) networks and the automated anatomical atlas (AAL), along with a selection of frequently utilized ROIs derived from recognized networks and areas (Yeo et al., 2011). Based on the task-relevant activation regions activated during the Stroop task performance, we defined the following brain regions as seed regions: the dorsal anterior cingulate cortex (dACC), bilateral anterior insula (aINS), rostral prefrontal cortex (rPFC), and supramarginal gyrus (SMG) as those involved in the salience network (SN); the lateral prefrontal cortex (lPFC) and posterior parietal cortex (PPC) as those involved in the CEN; and the medial prefrontal cortex and posterior cingulate cortex as those representing the DMN. Additionally, 10 bilateral ROIs in subcortical areas were selected, including the bilateral putamen, hippocampus, and three thalamic subdivisions (lateral geniculate nucleus [LGN], pulvinar, and mediodorsal nucleus of the thalamus [MD]). As the lPFC can be broadly subdivided into the dorsolateral PFC (dlPFC) and ventrolateral PFC (vlPFC), which approximately correspond to Brodmann areas (BA) 9/46 and 45/47, respectively, we also added BA 9 and 46 for the dlPFC and BA 45 and 47 for the vlPFC (Petrides, 2005).

To analyze the functional connectivity, we first preprocessed the fMRI time series from all voxels within the gray matter to minimize potential confounding factors. This involved regressing out six rigid motions as well as noise components originating from the white matter and cerebrospinal fluid masks. In addition, linear trends and cosine and sine waveforms up to 0.009 Hz were removed. Following the

preprocessing steps, functional connectivity was determined by calculating the correlation coefficients between the seed time series and those of all voxels in the entire brain during the task condition. To improve normality, the correlation coefficients were Fisher z-transformed. The z-scores of functional connectivity were averaged across voxels of interest for quantitative analysis. To evaluate the significance of seed-based functional connectivity regarding tACS phase differences, paired t-tests were performed with a voxel-level significance threshold set at $p < 0.001$ between congruent and incongruent trials within each tACS phase (i.e., 0°- and 180°-phase-lags). To address multiple comparisons, cluster-level FWE correction with a significance threshold set at $p < 0.05$ was applied during the cluster size analysis.

CRediT authorship contribution statement

Jeehye Seo: Writing – original draft, Visualization, Formal analysis, Data curation. **Jehyeop Lee:** Formal analysis, Visualization. **Byoung-Kyong Min:** Conceptualization, Data curation, Formal analysis, Funding acquisition, Investigation, Methodology, Project administration, Resources, Software, Supervision, Visualization, Writing – original draft, Writing – review & editing.

Declaration of competing interest

The authors declare no competing interests.

Data availability

The data and analysis codes used in this study are available from the corresponding author upon request.

Acknowledgments

We thank Je-Choon Park, Jeongwook Kwon, Yukyung Kim, Sangbin Yun, and Jaewon Yang for their assistance with fMRI data acquisition and tACS administration. We also thank Dr. Dongha Lee for his kind work in drawing Fig. 7. This work was supported by the Convergent Technology R&D Program for Human Augmentation (grant number 2020M3C1B8081319 to BK.M.), funded by the Korean government through the National Research Foundation of Korea.

References

Aizenstein, H.J., Butters, M.A., Clark, K.A., Figurski, J.L., Andrew Stenger, V., Nebes, R. D., Reynolds 3rd, C.F., Carter, C.S., 2006. Prefrontal and striatal activation in elderly subjects during concurrent implicit and explicit sequence learning. Neurobiol. Aging 27, 741–751.
Alekseichuk, I., Falchier, A.Y., Linn, G., Xu, T., Milham, M.P., Schroeder, C.E., Opitz, A., 2019. Electric field dynamics in the brain during multi-electrode transcranial electric stimulation. Nat. Commun. 10, 2573.
Alekseichuk, I., Pabel, S.C., Antal, A., Paulus, W., 2017. Intrahemispheric theta rhythm desynchronization impairs working memory. Restor. Neurol. Neurosci. 35, 147–158.
Alekseichuk, I., Wischnewski, M., Opitz, A., 2022. A minimum effective dose for (transcranial) alternating current stimulation. Brain Stimul. 15, 1221–1222. Basic, Translational, and Clinical Research in Neuromodulation.
Alexander, G.E., Crutcher, M.D., 1990. Preparation for movement: neural representations of intended direction in three motor areas of the monkey. J. Neurophysiol. 64, 133–150.
Angius, L., Santarnecchi, E., Pascual-Leone, A., Marcora, S.M., 2019. Transcranial direct current stimulation over the left dorsolateral prefrontal cortex improves inhibitory control and endurance performance in healthy individuals. Neuroscience 419, 34–45.
Apps, M.A., Balsters, J.H., Ramnani, N., 2012. The anterior cingulate cortex: monitoring the outcomes of others' decisions. Soc. Neurosci. 7, 424–435.
Aron, A.R., Robbins, T.W., Poldrack, R.A., 2014. Inhibition and the right inferior frontal cortex: one decade on. Trends Cogn. Sci. (Regul. Ed.) 18, 177–185.
Asamoah, B., Khatoun, A., Mc Laughlin, M., 2019. tACS motor system effects can be caused by transcutaneous stimulation of peripheral nerves. Nat. Commun. 10, 266.
Banich, M.T., 2009. Executive function: the search for an integrated account. Curr. Dir. Psychol. Sci. 18, 89–94.
Banich, M.T., 2019. The Stroop effect occurs at multiple points along a cascade of control: evidence from cognitive neuroscience approaches. Front. Psychol. 10, 2164.
Banich, M.T., Milham, M.P., Atchley, R.A., Cohen, N.J., Webb, A., Wszalek, T., Kramer, A.F., Liang, Z., Barad, V., Gullett, D., Shah, C., Brown, C., 2000. Prefrontal regions play a predominant role in imposing an attentional 'set': evidence from fMRI. Brain Res. Cogn. Brain Res. 10, 1–9.
Banich, M.T., Milham, M.P., Jacobson, B.L., Webb, A., Wszalek, T., Cohen, N.J., Kramer, A.F., 2001. Attentional selection and the processing of task-irrelevant information: insights from fMRI examinations of the Stroop task. Prog. Brain Res. 134, 459–470.
Benjamini, Y., Hochberg, Y., 1995. Controlling the false discovery rate: a practical and powerful approach to multiple testing. J. R. Stat. Soc. Ser. B (Methodological) 57, 289–300.
Bhattacharjee, S., Kashyap, R., Abualait, T., Annabel Chen, S.H., Yoo, W.K., Bashir, S., 2021. The role of primary motor cortex: more than movement execution. J. Mot. Behav. 53, 258–274.
Booth, J.R., Burman, D.D., Meyer, J.R., Lei, Z., Trommer, B.L., Davenport, N.D., Li, W., Parrish, T.B., Gitelman, D.R., Mesulam, M.M., 2003. Neural development of selective attention and response inhibition. Neuroimage 20, 737–751.
Borsa, V.M., Della Rosa, P.A., Catricala, E., Canini, M., Iadanza, A., Falini, A., Abutalebi, J., Iannaccone, S., 2018. Interference and conflict monitoring in individuals with amnestic mild cognitive impairment: a structural study of the anterior cingulate cortex. J. Neuropsychol. 12, 23–40.
Botvinick, M.M., 2007. Conflict monitoring and decision making: reconciling two perspectives on anterior cingulate function. Cogn. Affect. Behav. Neurosci. 7, 356–366.
Botvinick, M.M., Braver, T.S., Barch, D.M., Carter, C.S., Cohen, J.D., 2001. Conflict monitoring and cognitive control. Psychol. Rev. 108, 624–652.
Botvinick, M.M., Cohen, J.D., Carter, C.S., 2004. Conflict monitoring and anterior cingulate cortex: an update. Trends. Cogn. Sci. 8, 539–546.
Brunoni, A.R., Vanderhasselt, M.A., 2014. Working memory improvement with non-invasive brain stimulation of the dorsolateral prefrontal cortex: a systematic review and meta-analysis. Brain Cogn. 86, 1–9.
Brunye, T.T., Moran, J.M., Holmes, A., Mahoney, C.R., Taylor, H.A., 2017. Non-invasive brain stimulation targeting the right fusiform gyrus selectively increases working memory for faces. Brain Cogn. 113, 32–39.
Bullmore, E., Brammer, M., Williams, S.C., Rabe-Hesketh, S., Janot, N., David, A., Mellers, J., Howard, R., Sham, P., 1996. Statistical methods of estimation and inference for functional MR image analysis. Magn. Reson. Med. 35, 261–277.
Bush, G., Luu, P., Posner, M.I., 2000. Cognitive and emotional influences in anterior cingulate cortex. Trends. Cogn. Sci. 4, 215–222.
Casey, B., Durston, S., Fossella, J.A., 2001. Evidence for a mechanistic model of cognitive control. Clin. Neurosci. Res. 1, 267–282.
Cavanagh, J.F., Frank, M.J., 2014. Frontal theta as a mechanism for cognitive control. Trends. Cogn. Sci. 18, 414–421.
Chand, G.B., Dhamala, M., 2016. Interactions among the brain default-mode, salience, and central-executive networks during perceptual decision-making of moving dots. Brain Connect. 6, 249–254.
Cohen, M.X., Cavanagh, J.F., 2011. Single-trial regression elucidates the role of prefrontal theta oscillations in response conflict. Front. Psychol. 2, 30.
Cohen, M.X., Donner, T.H., 2013. Midfrontal conflict-related theta-band power reflects neural oscillations that predict behavior. J. Neurophysiol. 110, 2752–2763.
Craig, A.D., 2009. How do you feel—now? The anterior insula and human awareness. Nat. Rev. Neurosci. 10, 59–70.
De Boeck, P., Jeon, M., 2019. An overview of models for response times and processes in cognitive tests. Front. Psychol. 10, 102.
Diamond, A., 2013. Executive functions. Annu. Rev. Psychol. 64, 135–168.
Doesburg, S.M., Green, J.J., McDonald, J.J., Ward, L.M., 2009. From local inhibition to long-range integration: a functional dissociation of alpha-band synchronization across cortical scales in visuospatial attention. Brain Res. 1303, 97–110.
Dosenbach, N.U., Fair, D.A., Miezin, F.M., Cohen, A.L., Wenger, K.K., Dosenbach, R.A., Fox, M.D., Snyder, A.Z., Vincent, J.L., Raichle, M.E., 2007. Distinct brain networks for adaptive and stable task control in humans. Proc. Natl. Acad. Sci. 104, 11073–11078.
Egner, T., Hirsch, J., 2005. Cognitive control mechanisms resolve conflict through cortical amplification of task-relevant information. Nat. Neurosci. 8, 1784–1790.
Esmaeilpour, Z., Kronberg, G., Reato, D., Parra, L.C., Bikson, M., 2021. Temporal interference stimulation targets deep brain regions by modulating neural oscillations. Brain Stimul. 14, 55–65.
Filmer, H.L., Dux, P.E., Mattingley, J.B., 2014. Applications of transcranial direct current stimulation for understanding brain function. Trends. Neurosci. 37, 742–753.
Fox, M.D., Corbetta, M., Snyder, A.Z., Vincent, J.L., Raichle, M.E., 2006. Spontaneous neuronal activity distinguishes human dorsal and ventral attention systems. Proc. Natl. Acad. Sci. 103, 10046–10051.
Fox, N.A., Calkins, S.D., 2003. The development of self-control of emotion: intrinsic and extrinsic influences. Motiv. Emot. 27, 7–26.
Friedman, N.P., Miyake, A., 2004. The relations among inhibition and interference control functions: a latent-variable analysis. J. Exp. Psychol. Gen. 133, 101.
Fries, P., 2005. A mechanism for cognitive dynamics: neuronal communication through neuronal coherence. Trends. Cogn. Sci. 9, 474–480.
Fujiyama, H., Van Soom, J., Rens, G., Cuypers, K., Heise, K.F., Levin, O., Swinnen, S.P., 2016. Performing two different actions simultaneously: the critical role of interhemispheric interactions during the preparation of bimanual movement. Cortex 77, 141–154.
Fuster, J.M., 2001. The prefrontal cortex–an update: time is of the essence. Neuron 30, 319–333.

Goghari, V.M., MacDonald III, A.W., 2009. The neural basis of cognitive control: response selection and inhibition. Brain Cogn. 71, 72–83.
Gollo, L.L., Mirasso, C., Sporns, O., Breakspear, M., 2014. Mechanisms of zero-lag synchronization in cortical motifs. PLoS. Comput. Biol. 10, e1003548.
Greicius, M.D., Krasnow, B., Reiss, A.L., Menon, V., 2003. Functional connectivity in the resting brain: a network analysis of the default mode hypothesis. Proc. Natl. Acad. Sci. 100, 253–258.
Grinband, J., Hirsch, J., Ferrera, V.P., 2006. A neural representation of categorization uncertainty in the human brain. Neuron 49, 757–763.
Grossman, N., Bono, D., Dedic, N., Kodandaramaiah, S.B., Rudenko, A., Suk, HJ., Cassara, A.M., Neufeld, E., Kuster, N., Tsai, LH., 2017. Noninvasive deep brain stimulation via temporally interfering electric fields. Cell 169, 1029–1041 e1016.
Guo, Y., Schmitz, T.W., Mur, M., Ferreira, C.S., Anderson, M.C., 2018. A supramodal role of the basal ganglia in memory and motor inhibition: meta-analytic evidence. Neuropsychologia 108, 117–134.
Halassa, M.M., Acsády, L., 2016. Thalamic inhibition: diverse sources, diverse scales. Trends Neurosci. 39, 680–693.
Halassa, M.M., Kastner, S., 2017. Thalamic functions in distributed cognitive control. Nat. Neurosci. 20, 1669–1679.
Hanslmayr, S., Pastotter, B., Bauml, K.H., Gruber, S., Wimber, M., Klimesch, W., 2008. The electrophysiological dynamics of interference during the Stroop task. J. Cogn. Neurosci. 20, 215–225.
Helfrich, R.F., Schneider, T.R., Rach, S., Trautmann-Lengsfeld, S.A., Engel, A.K., Herrmann, C.S., 2014. Entrainment of brain oscillations by transcranial alternating current stimulation. Curr. Biol. 24, 333–339.
Hendry, A., Agyapong, M.A., D'Souza, H., Frick, M.A., Portugal, A.M., Konke, L.A., Cloke, H., Bedford, R., Smith, T.J., Karmiloff-Smith, A., Jones, E.J.H., Charman, T., Brocki, K.C., 2022. Inhibitory control and problem solving in early childhood: exploring the burdens and benefits of high self-control. Infant. Child Dev. 31, e2297.
Herrmann, C.S., Rach, S., Neuling, T., Struber, D., 2013. Transcranial alternating current stimulation: a review of the underlying mechanisms and modulation of cognitive processes. Front. Hum. Neurosci. 7, 279.
Hill, A.T., Rogasch, N.C., Fitzgerald, P.B., Hoy, K.E., 2019. Impact of concurrent task performance on transcranial direct current stimulation (tDCS)-Induced changes in cortical physiology and working memory. Cortex 113, 37–57.
Huang, W.A., Stitt, I.M., Negahbani, E., Passey, D., Ahn, S., Davey, M., Dannhauer, M., Doan, T.T., Hoover, A.C., Peterchev, A.V., 2021. Transcranial alternating current stimulation entrains alpha oscillations by preferential phase synchronization of fast-spiking cortical neurons to stimulation waveform. Nat. Commun. 12, 3151.
Johnson, L., Alekseichuk, I., Krieg, J., Doyle, A., Yu, Y., Vitek, J., Johnson, M., Opitz, A., 2020. Dose-dependent effects of transcranial alternating current stimulation on spike timing in awake nonhuman primates. Sci. Adv. 6, eaaz2747.
Johnston, K., Levin, H.M., Koval, M.J., Everling, S., 2007. Top-down control-signal dynamics in anterior cingulate and prefrontal cortex neurons following task switching. Neuron 53, 453–462.
Kerns, J.G., Cohen, J.D., MacDonald 3rd, A.W., Cho, R.Y., Stenger, V.A., Carter, C.S., 2004. Anterior cingulate conflict monitoring and adjustments in control. Science (1979) 303, 1023–1026.
Khan, A., Mosbacher, J.A., Vogel, S.E., Binder, M., Wehovz, M., Moshammer, A., Halverscheid, S., Pustelnik, K., Nitsche, M.A., Tong, R.K., Grabner, R.H., 2023. Modulation of resting-state networks following repetitive transcranial alternating current stimulation of the dorsolateral prefrontal cortex. Brain Struct. Funct. 228, 1643–1655.
Kim, SE., Kim, HS., Kwak, Y., Ahn, MH., Choi, K.M., Min, BK., 2022. Neurodynamic correlates for the cross-frequency coupled transcranial alternating current stimulation during working memory performance. Front. Neurosci. 16, 1013691.
Koster, R., Guitart-Masip, M., Dolan, R.J., Duzel, E., 2015. Basal ganglia activity mirrors a benefit of action and reward on long-lasting event memory. Cereb. Cortex. 25, 4908–4917.
Krause, M.R., Vieira, P.G., Csorba, B.A., Pilly, P.K., Pack, C.C., 2019. Transcranial alternating current stimulation entrains single-neuron activity in the primate brain. Proc. Natl. Acad. Sci. U S A 116, 5747–5755.
Krug, M.K., Carter, C.S., 2012. Conflict control loop theory of cognitive control. In: Mangun, G.R. (Ed.), The Neuroscience of Attention: Attentional Control and Selection. Oxford University Press.
Lehr, A., Henneberg, N., Nigam, T., Paulus, W., Antal, A., 2019. Modulation of conflict processing by theta-range tACS over the dorsolateral prefrontal cortex. Neural Plast., 6747049, 2019.
Levasseur-Moreau, J., Fecteau, S., 2012. Translational application of neuromodulation of decision-making. Brain Stimul. 5, 77–83.
Loftus, A.M., Yalcin, O., Baughman, F.D., Vanman, E.J., Hagger, M.S., 2015. The impact of transcranial direct current stimulation on inhibitory control in young adults. Brain Behav. 5, e00332.
MacDonald 3rd, A.W., Cohen, J.D., Stenger, V.A., Carter, C.S., 2000. Dissociating the role of the dorsolateral prefrontal and anterior cingulate cortex in cognitive control. Science (1979) 288, 1835–1838.
Maciejewski, D., Lauharatanahirun, N., Herd, T., Lee, J., Deater-Deckard, K., King-Casas, B., Kim-Spoon, J., 2018. Neural cognitive control moderates the association between insular risk processing and risk-taking behaviors via perceived stress in adolescents. Dev. Cogn. Neurosci. 30, 150–158.
MacLeod, C.M., MacDonald, P.A., 2000. Interdimensional interference in the Stroop effect: uncovering the cognitive and neural anatomy of attention. Trends. Cogn. Sci. 4, 383–391.
Mansouri, F., Shanbour, A., Mazza, F., Fettes, P., Zariffa, J., Downar, J., 2019. Effect of theta transcranial alternating current stimulation and phase-locked transcranial pulsed current stimulation on learning and cognitive control. Front. Neurosci. 13, 1181.
Marchand, W.R., Lee, J.N., Thatcher, J.W., Hsu, E.W., Rashkin, E., Suchy, Y., Chelune, G., Starr, J., Barbera, S.S., 2008. Putamen coactivation during motor task execution. Neuroreport 19, 957–960.
Menon, V., 2011. Large-scale brain networks and psychopathology: a unifying triple network model. Trends Cogn. Sci. (Regul. Ed.) 15, 483–506.
Menon, V., D'Esposito, M., 2022. The role of PFC networks in cognitive control and executive function. Neuropsychopharmacology 47, 90–103.
Menon, V., Uddin, L.Q., 2010. Saliency, switching, attention and control: a network model of insula function. Brain Struct. Funct. 214, 655–667.
Michael, G.A., Buron, V., 2005. The human pulvinar and stimulus-driven attentional control. Behav. Neurosci. 119, 1353.
Miller, E.K., Cohen, J.D., 2001. An integrative theory of prefrontal cortex function. Annu Rev. Neurosci. 24, 167–202.
Min, BK., Kim, H.S., Pinotsis, D.A., Pantazis, D., 2020. Thalamocortical inhibitory dynamics support conscious perception. Neuroimage 220, 117066.
Monchi, O., Petrides, M., Strafella, A.P., Worsley, K.J., Doyon, J., 2006. Functional role of the basal ganglia in the planning and execution of actions. Ann. Neurol. 59, 257–264.
Nee, D.E., Wager, T.D., Jonides, J., 2007. Interference resolution: insights from a meta-analysis of neuroimaging tasks. Cogn. Affect. Behav. Neurosci. 7, 1–17.
Nekovarova, T., Fajnerova, I., Horacek, J., Spaniel, F., 2014. Bridging disparate symptoms of schizophrenia: a triple network dysfunction theory. Front. Behav. Neurosci. 8, 171.
Nigbur, R., Cohen, M.X., Ridderinkhof, K.R., Sturmer, B., 2012. Theta dynamics reveal domain-specific control over stimulus and response conflict. J. Cogn. Neurosci. 24, 1264–1274.
Oehrn, C.R., Hanslmayr, S., Fell, J., Deuker, L., Kremers, N.A., Do Lam, A.T., Elger, C.E., Axmacher, N., 2014. Neural communication patterns underlying conflict detection, resolution, and adaptation. J. Neurosci. 34, 10438–10452.
Palva, S., Palva, J.M., 2011. Functional roles of alpha-band phase synchronization in local and large-scale cortical networks. Front. Psychol. 2, 204.
Peters, S.K., Dunlop, K., Downar, J., 2016. Cortico-striatal-thalamic loop circuits of the salience network: a central pathway in psychiatric disease and treatment. Front. Syst. Neurosci. 10, 104.
Petrides, M., 2005. Lateral prefrontal cortex: architectonic and functional organization. Philos. Trans. R. Soc. Lond. B Biol. Sci. 360, 781–795.
Phillips, J.M., Kambi, N.A., Redinbaugh, M.J., Mohanta, S., Saalmann, Y.B., 2021. Disentangling the influences of multiple thalamic nuclei on prefrontal cortex and cognitive control. Neurosci. Biobehav. Rev. 128, 487–510.
Polanía, R., Krajbich, I., Grueschow, M., Ruff, C.C., 2014. Neural oscillations and synchronization differentially support evidence accumulation in perceptual and value-based decision making. Neuron 82, 709–720.
Polanía, R., Moisa, M., Opitz, A., Grueschow, M., Ruff, C.C., 2015. The precision of value-based choices depends causally on fronto-parietal phase coupling. Nat. Commun. 6, 1–10.
Polania, R., Nitsche, M.A., Korman, C., Batsikadze, G., Paulus, W., 2012. The importance of timing in segregated theta phase-coupling for cognitive performance. Curr. Biol. 22, 1314–1318.
Polk, T.A., Drake, R.M., Jonides, J.J., Smith, M.R., Smith, E.E., 2008. Attention enhances the neural processing of relevant features and suppresses the processing of irrelevant features in humans: a functional magnetic resonance imaging study of the Stroop task. J. Neurosci. 28, 13786–13792.
Pulopulos, M.M., Schmausser, M., De Smet, S., Vanderhasselt, M.A., Baliyan, S., Venero, C., Baeken, C., De Raedt, R., 2020. The effect of HF-rTMS over the left DLPFC on stress regulation as measured by cortisol and heart rate variability. Horm. Behav. 124, 104803.
Purmann, S., Pollmann, S., 2015. Adaptation to recent conflict in the classical color-word Stroop-task mainly involves facilitation of processing of task-relevant information. Front. Hum. Neurosci. 9, 88.
Raichle, M.E., MacLeod, A.M., Snyder, A.Z., Powers, W.J., Gusnard, D.A., Shulman, G.L., 2001a. A default mode of brain function. Proc. Natl. Acad. Sci. 98, 676–682.
Raichle, M.E., MacLeod, A.M., Snyder, A.Z., Powers, W.J., Gusnard, D.A., Shulman, G.L., 2001b. A default mode of brain function. Proc. Natl. Acad. Sci. U S A 98, 676–682.
Reato, D., Rahman, A., Bikson, M., Parra, L.C., 2010. Low-intensity electrical stimulation affects network dynamics by modulating population rate and spike timing. J. Neurosci. 30, 15067–15079.
Reinhart, R.M.G., 2017. Disruption and rescue of interareal theta phase coupling and adaptive behavior. Proc. Natl. Acad. Sci. U S A 114, 11542–11547.
Salvia, E., Tissier, C., Charron, S., Herent, P., Vidal, J., Lion, S., Cassotti, M., Oppenheim, C., Houde, O., Borst, G., Cachia, A., 2019. The local properties of bold signal fluctuations at rest monitor inhibitory control training in adolescents. Dev. Cogn. Neurosci. 38, 100664.
Schluter, R.S., Daams, J.G., van Holst, R.J., Goudriaan, A.E., 2018. Effects of non-invasive neuromodulation on executive and other cognitive functions in addictive disorders: a systematic review. Front. Neurosci. 12, 642.
Schutter, D.J., 2016. Cutaneous retinal activation and neural entrainment in transcranial alternating current stimulation: a systematic review. Neuroimage 140, 83–88.
Seeley, W.W., Menon, V., Schatzberg, A.F., Keller, J., Glover, G.H., Kenna, H., Reiss, A.L., Greicius, M.D., 2007. Dissociable intrinsic connectivity networks for salience processing and executive control. J. Neurosci. 27, 2349–2356.
Seo, J., Kim, DJ., Choi, SH., Kim, H., Min, BK., 2022. The thalamocortical inhibitory network controls human conscious perception. Neuroimage 264, 119748.
Shenhav, A., Botvinick, M.M., Cohen, J.D., 2013. The expected value of control: an integrative theory of anterior cingulate cortex function. Neuron 79, 217–240.

Siegrist, M., 1997. Test-retest reliability of different versions of the Stroop test. J. Psychol. 131, 299–306.
Silton, R.L., Heller, W., Towers, D.N., Engels, A.S., Spielberg, J.M., Edgar, J.C., Sass, S.M., Stewart, J.L., Sutton, B.P., Banich, M.T., Miller, G.A., 2010. The time course of activity in dorsolateral prefrontal cortex and anterior cingulate cortex during top-down attentional control. Neuroimage 50, 1292–1302.
Sormaz, M., Murphy, C., Wang, H.T., Hymers, M., Karapanagiotidis, T., Poerio, G., Margulies, D.S., Jefferies, E., Smallwood, J., 2018. Default mode network can support the level of detail in experience during active task states. Proc. Natl. Acad. Sci. U S A 115, 9318–9323.
Sridharan, D., Levitin, D.J., Menon, V., 2008. A critical role for the right fronto-insular cortex in switching between central-executive and default-mode networks. Proc. Natl. Acad. Sci. 105, 12569–12574.
Strauss, E., Sherman, E.M., Spreen, O., 2006. A Compendium of Neuropsychological Tests: Administration, Norms, and Commentary. American Chemical Society.
Stroop, J.R., 1935. Studies of interference in serial verbal reactions. J. Exp. Psychol. 18, 643–662.
Swick, D., Ashley, V., Turken, U., 2011. Are the neural correlates of stopping and not going identical? Quantitative meta-analysis of two response inhibition tasks. Neuroimage 56, 1655–1665.
Theeuwes, J., 2010. Top-down and bottom-up control of visual selection. Acta Psychol. (Amst) 135, 77–99.
Thielscher, A., Antunes, A., Saturnino, G.B., 2015. Field modeling for transcranial magnetic stimulation: a useful tool to understand the physiological effects of TMS?. In: Proceedings of the 37th Annual International Conference of the IEEE Engineering in Medicine And Biology Society (EMBC). IEEE, pp. 222–225.
Thut, G., Miniussi, C., 2009. New insights into rhythmic brain activity from TMS-EEG studies. Trends. Cogn. Sci. 13, 182–189.
Tseng, P., Iu, K.C., Juan, C.H., 2018. The critical role of phase difference in theta oscillation between bilateral parietal cortices for visuospatial working memory. Sci. Rep. 8, 349.
Uddin, L.Q., Menon, V., 2009. The anterior insula in autism: under-connected and under-examined. Neurosci. Biobehav. Rev. 33, 1198–1203.
Ullsperger, M., Harsay, H.A., Wessel, J.R., Ridderinkhof, K.R., 2010. Conscious perception of errors and its relation to the anterior insula. Brain Struct. Funct. 214, 629–643.
Vanderhasselt, M.A., De Raedt, R., Baeken, C., 2009. Dorsolateral prefrontal cortex and Stroop performance: tackling the lateralization. Psychon. Bull. Rev. 16, 609–612.
Veniero, D., Strüber, D., Thut, G., Herrmann, C.S., 2019. Noninvasive brain stimulation techniques can modulate cognitive processing. Organ. Res. Methods 22, 116–147.
Violante, I.R., Li, L.M., Carmichael, D.W., Lorenz, R., Leech, R., Hampshire, A., Rothwell, J.C., Sharp, D.J., 2017. Externally induced frontoparietal synchronization modulates network dynamics and enhances working memory performance. Elife 6.
Volpe, G., Tagliente, S., Palmisano, A., Grattagliano, I., Rivolta, D., 2022. Non-invasive neuromodulation can reduce aggressive behaviors in humans: a critical perspective. J. Forensic Sci. 67, 1593–1606.
Voytek, B., Knight, R.T., 2010. Prefrontal cortex and basal ganglia contributions to visual working memory. Proc. Natl. Acad. Sci. U S A 107, 18167–18172.
Ward, A.M., Schultz, A.P., Huijbers, W., Van Dijk, K.R., Hedden, T., Sperling, R.A., 2014. The parahippocampal gyrus links the default-mode cortical network with the medial temporal lobe memory system. Hum. Brain Mapp. 35, 1061–1073.
Whitfield-Gabrieli, S., Nieto-Castanon, A., 2012. Conn: a functional connectivity toolbox for correlated and anticorrelated brain networks. Brain Connect. 2, 125–141.
Wischnewski, M., Tran, H., Zhao, Z., Shirinpour, S., Haigh, Z.J., Rotteveel, J., Perera, N. D., Alekseichuk, I., Zimmermann, J., Opitz, A., 2024. Induced neural phase precession through exogenous electric fields. Nat. Commun. 15, 1687.
Yeo, B.T., Krienen, F.M., Sepulcre, J., Sabuncu, M.R., Lashkari, D., Hollinshead, M., Roffman, J.L., Smoller, J.W., Zollei, L., Polimeni, J.R., Fischl, B., Liu, H., Buckner, R. L., 2011. The organization of the human cerebral cortex estimated by intrinsic functional connectivity. J. Neurophysiol. 106, 1125–1165.
Yeung, N., Botvinick, M.M., Cohen, J.D., 2004. The neural basis of error detection: conflict monitoring and the error-related negativity. Psychol. Rev. 111, 931–959.